Separation Science and Technology
Publication details, including instructions for authors and subscription information:
http://www.informaworld.com/smpp/title~content=t713708471

Characterization of Pd-Composite Membrane Fabricated by Surfactant Induced Electroless Plating (SIEP): Effect of Grain Size on Hydrogen Permeability

Mohammad A. Islam*[a]; Shamsuddin Ilias[a]
[a] Department of Chemical and Bioengineering, North Carolina A&T State University, Greensboro, NC, USA

To cite this Article Islam*, Mohammad A. and Ilias, Shamsuddin(2010) 'Characterization of Pd-Composite Membrane Fabricated by Surfactant Induced Electroless Plating (SIEP): Effect of Grain Size on Hydrogen Permeability', Separation Science and Technology, 45: 12, 1886 — 1893

To link to this Article: DOI: 10.1080/01496395.2010.493823

URL: http://dx.doi.org/10.1080/01496395.2010.493823

Separation Science and Technology, 45: 1886–1893, 2010
Copyright © Taylor & Francis Group, LLC
ISSN: 0149-6395 print/1520-5754 online
DOI: 10.1080/01496395.2010.493823

Characterization of Pd-Composite Membrane Fabricated by Surfactant Induced Electroless Plating (SIEP): Effect of Grain Size on Hydrogen Permeability

Mohammad A. Islam* and Shamsuddin Ilias
Department of Chemical and Bioengineering, North Carolina A&T State University, Greensboro, NC, USA

Polycrystalline palladium (Pd) was deposited on micro-porous stainless steel (MPSS) substrate using a suitable surfactant of various concentrations in the electroless plating process. The microstructural characterization was carried out using Scanning Electron Microscopy (SEM), Energy Dispersive Spectroscopy (EDS), and X-ray diffraction (XRD). The concentrations of the surfactant were chosen as a function of critical micelle concentration (CMC) in order to elucidate the interaction of the surfactant in solid-liquid and solid-gas interface during grain coarsening. It appears that during electro-crystallization, the driving force between the newly formed crystallite and the originally coarsed grains depends on the relative size and crystalline configuration of the newly formed crystallite. This crystallite on the other hand is affected by the localized over potential, the presence of active nucleating particles, and the texture of MPSS surface and operating conditions. The size of the newly formed grain is smaller when the concentration of the surface-active agents is relatively higher. It suggests that the surfactant active polar group inherently participates in the reaction/deposition process and effectively activates the process of grain nucleation and agglomeration in electro-crystallization. The membranes of different grain sizes were fabricated in the presence of the cationic surfactant DTAB (dodecyltrimethyiammonium bromide) of various concentrations. DTAB concentration is expressed in critical micelle concentration (CM), which ranged from CMC $\times \frac{1}{2}$ to CMC $\times$ 4. Fabricated membranes of different grain size and distribution were also studied for hydrogen permeability and selectivity. Results show that membranes with agglomerated grains (higher grain size) possess relatively higher permeability and selectivity.

Keywords critical micelle concentration; electroless plating; H_2-selectivity; H_2-separation; Pd membrane; permeability; surfactant

INTRODUCTION

Dense metallic membranes, especially palladium (Pd), and its alloy membranes exhibit extremely high selectivity for hydrogen. Hydrogen (H_2) permeation through these membranes proceeds via a solution-diffusion mechanism (1). Because of the comparatively low mechanical strength of Pd, Pd membranes cannot be reduced in thickness beyond a certain degree (2). As a result, H_2-flux through dense Pd membranes is small compared with those of microporous glass membranes.

To improve the perm-selectivity of the palladium membranes, a very thin film with structural integrity and thermal stability must be obtained. The system must possess sufficient mechanical integrity to operate at high transmembrane pressures. This can be achieved by preparing a composite membrane consisting of a highly selective skin layer membrane (Pd-film) attached to a thermally stable microporous inorganic substrate. The inorganic substrate provides the mechanical integrity while the skin layer membrane provides the selectivity.

In this context, deposition of a Pd/Pd-alloy thin film on microporous ceramic or stainless steel substrates for fabricating H_2-selective membrane for high temperature gas separations and membrane reactors have been studied extensively over the past two decades. There are various techniques by which a thin film of metal or metal-alloy may be deposited onto a ceramic substrate. Of all the methods, the electroless plating (EP) method for thin film deposition is generally preferred over other methods such as chemical vapor deposition (CVD), physical vapor deposition (PVD), and radio frequency (RF) cathodic sputtering. However, each of the methods has advantages and disadvantages.

Jayaraman et al. (3) fabricated ultrathin Pd film on a mesoporous ceramic substrate by radio frequency (RF) magnetron sputtering. Pd films under 500 nm thicknesses showed poor adhesion to the ceramic substrate. Hydrogen to nitrogen selectivity of these films was about 5.7 and attributed to pinholes in the ultrathin films (4). Bryden and Ying (5) investigated the H_2 permeation characteristics of nanostructured Pd membrane deposited on vycor glass using RF magnetron sputtering. Defect-free,

---

Received 25 October 2009; accepted 13 April 2010.

*Current Address: Aspen Technology, Inc., 2500 City West Blvd., Houston, TX 77042.

Address correspondence to Shamsuddin Ilias, Department of Chemical and Bioengineering, North Carolina A&T State University, Greensboro, NC 27411, USA. E-mail: ilias@ncat.edu

nanostructured Pd membranes generally possess higher H_2 permeability than conventional polycrystalline Pd due to their larger volume fraction of grain boundaries.

Xomeritakis and Lin (6) prepared thin Pd-film (0.5–5.0 μm) on sol-gel derived γ-alumina supports by CVD and reported that the H_2-permeance is strongly influenced by the Pd crystallinity and morphology. The H_2-permeance increased with the Pd grain size. The vacuum assisted electrodeposition technique has been used to fabricate Pd-Ni alloy membranes on stainless steel support with an intermediate TiN diffusion barrier between the Pd-Ni active layer and support. The Pd-Ni composite membrane showed excellent perm-selectivity for H_2 with thermal stability for over 60 days (7).

The electroless plating method has been extensively used in fabricating Pd and Pd-alloy composite membranes for high temperature H_2-separation applications (8–16).

This method offers some advantages over other methods, such as:

1. it can be applied on both conducting and non-conducting surfaces,
2. it can be applied to substrate of any size and shape, and
3. the plating bath set-up is simple and relatively inexpensive.

Electroless plating of Pd is a combination of cathodic deposition of metal and anodic oxidation of reductant in an immersion potential. The conventional electroless plating (CEP) process is greatly limited by the formation of dendritic structures throughout the target surface that result in non-uniformity in the deposition morphology and microstructure. Barton and Bockris (17) investigated the electrolytic growth of ionic dendrite formation in Ag^+ deposition. Dendrite formation depends on factors such as overpotential, pH, concentration of existing ions and temperature (17). In conventional Pd electroless plating, similar factors affect the dendrite formation (18). Dendritic growth of Pd crystallites during electroless plating hinders formation of uniform Pd film on porous substrate. The long-term performance of the Pd-composite membrane fabricated by the electroless plating is greatly affected by the crystallite distribution and microstructural characteristics of the film (11).

In CEP, oxidation-reduction reactions between Pd-complex and hydrazine (reducing agent) results in metallic deposition of Pd° in a solid surface. An efficient electron transfer between the phases is very imperative in dense film layer deposition. The surface morphology of the substrate controls the size of Pd grains and degree of agglomeration. The oxidation-reduction reactions between Pd-complex and hydrazine result in evolution of ammonia and nitrogen gas bubbles during the electroless plating process. When adhering to the substrate surface and in the pores, these gas bubbles hinder uniform Pd-film deposition which results in dendrite growth. To address the problem associated with the bubbles in the plating substrate vicinity, the role of surface active agents with favorable structures in the electroless plating process was explored (19). In our new approach presented here, surfactant-induced electroless plating (SIEP), the deposited Pd grain size, and subsequent agglomeration have been manipulated and tailored using suitable surfactants. In this paper, the deposition of polycrystalline Pd on a micro-porous stainless steel (MPSS) substrate using SIEP with a cationic surfactant is reported.

MATERIALS AND METHODS

All MPSS substrate discs of 1/8th-inch thickness and 1-inch diameter with nominal pore size of 0.2 μm used in this study were obtained from Mott Metallurgical Corporation. The manufacturer's product information is used to determine the average pore size of the substrate. Before sensitization and activation, the MPSS disc substrate was thoroughly cleaned and dried using carbon tetrachloride and ethanol (Fisher Scientific, ACS reagent grade). The sensitization and activation solutions were prepared using reagent grade $SnCl_2$(Sigma Aldrich, 98%) and $PdCl_2$(Sigma Aldrich, 99.9%) in hydrochloric acid. The composition of the sensitization and activation solutions is given in Table 1.

The deposition of Pd on the Sn/Pd-activated MPSS disc was carried out in an electroless plating bath at a constant temperature of 55°C. The details are discussed elsewhere. The composition and operating conditions of the Pd electroless plating bath used in this study is given in Table 2. Analytical grade ammonium hydroxide and hydrazine (1.0 M) were obtained from Arcos Organic. EDTA sodium salt and tetra-amine palladium nitrate were supplied by Sigma Aldrich. Cationic surfactant DTAB (dodecytrimethylammonium bromide, MW 308.35) was also obtained from Sigma Aldrich. To study the role of DTAB in Pd-deposition, DTAB concentration was varied over a wide range. Surfactant concentration is expressed in critical micelle concentration (CMC). The DTAB concentration ranged from CMC $\times \frac{1}{2}$, to CMC $\times 4$.

The microstructure of Pd membranes was analyzed using scanning electron microscopy (SEM), energy dispersive spectroscopy (EDS), X-ray diffraction (XRD), and atomic force microscopy (AFM). Grain sizes were determined using point-to-point measurements from

TABLE 1
Composition of sensitization and activation solutions

Sensitization solution		Activation solution	
Component	Concentration	Component	Concentration
$SnCl_2$	1.19 g/l	$PdCl_2$	0.09 g/l
HCl	0.2 N	HCl	0.2 N

TABLE 2
Electroless plating bath composition used in Pd-membrane fabrications

Compositions	Concentrations
Ammonium hydroxide (28%)	198 ml/l
Hydrazine (1.0 M)	5.6–6.7 mM
Tetra-amine palladium nitrate (10 w %)	15.6 mM
EDTA sodium salt	40.1 g/l
DTAB	CMC†
Operating conditions	
Temperature	55°C
pH	10–11

†Various surfactants were added based on their critical micelle concentration (CMC).

representative SEM images. Statistical distributions were estimated considering a minimum of 1000 grains in a constant cross-section area. Membranes were fabricated using different DTAB concentrations under identical plating bath conditions. Pd-MPSS membrane gas tightness and H_2-permeability and selectivity studies were carried out in the in-house built diffusivity measurement setup (20).

RESULTS AND DISCUSSION

To elucidate the role of cationic surfactant (DTAB) in electroless plating, Pd-composite membranes were prepared on MPSS at DTAB concentrations ranging from no-CMC to CMC × 4. Table 3 shows the Pd-film thickness and electroless plating time for each of the membranes at corresponding DTAB CMC. Pd-film thickness was estimated using both weight-gain and SEM analysis of Pd-composite membrane cross-section. Estimated film thicknesses were very comparable by the two methods. As shown in Table 3, it can be observed that with increased DTAB concentration thinner Pd-film can be fabricated with a significant reduction in the plating time. Membrane thickness varies linearly with electroless plating time. The correlation coefficients (R^2) of the linear fit were found to be 0.97 and 0.96 for film thickness determined by weight-gain and SEM analysis, respectively. In the presence of DTAB, a thinner membrane could be fabricated in a shorter time.

TABLE 3
Measured Pd-film thickness by weight-gain method and SEM x-section analysis of SIEP MPSS-Pd composite membranes

Membrane sample	DTAB concentration (CMC)	Deposition time (h)	Pd-film thickness (μm) measured by	
			Weight-gain	SEM analysis
A	0.5	22	23.0	22.5
B	2	16	17.8	18.3
C	3	13	14.0	13.5
D	4	10	8.5	8.5
E	0	28	28.5	27.5

The gas-tightness of these membranes was tested for helium transport at a transmembrane pressure and temperature of 625 kPa and 300 K, respectively. Helium was chosen for gas-tightness testing for being the smaller molecule (2.6 Å) compared to hydrogen (2.89 Å). In Fig. 1, the helium flow rate as a function of Pd-film thickness is shown at various DTAB CMCs. The results show that to obtain a gas-tight Pd-composite membrane, a Pd-film deposit of as much as 25 μm or more in the absence of any DTAB in the electroless plating process may have to be used. However, using DTAB in the electroless plating process a thinner Pd-composite membrane with significantly improved gas-tightness can be easily fabricated. In fact at CMC × 4, helium-tight Pd-composite membranes with film thicknesses of 10 μm or less were fabricated in this study (Fig. 1).

To illustrate the role of DTAB in Pd-film formation, the SEM images of two membranes at CMC × 2 and CMC × 4 are compared with a membrane fabricated without any

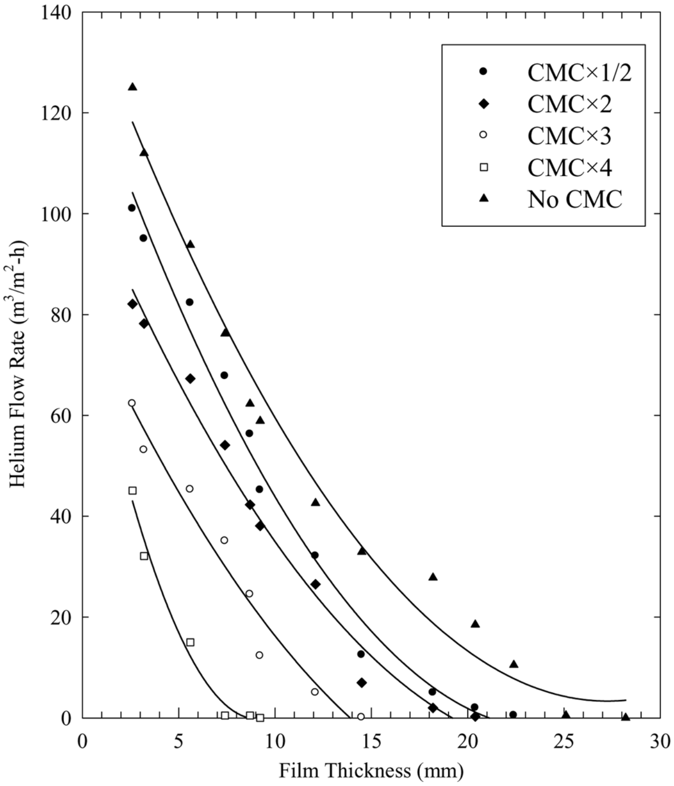

FIG. 1. Helium flow rate as a function of Pd-film thickness of different membranes fabricated at varied CMCs of DTAB surfactant.

DTAB in the electroless plating process, as shown in Fig. 2. SEM images of each of the membranes are shown at two different magnifications (5 k and 15 k). The presence of the surfactant at varying CMCs influences deposited Pd-grain size and its subsequent agglomeration. As shown in Fig. 2, as the surfactant concentration increases, the grain size becomes finer. As a result, the film structure becomes more continuous and uniform. In the absence of DTAB, SEM images clearly show the non-diffused grain and grain boundaries that are responsible for intra- or inter-granular porosity of the film (Fig. 2a). At CMC × 2 and CMC × 4, the grain boundaries diffuse and the resulting film appears smooth (Fig. 2b and 2c). Based on the gas-tightness tests (Fig. 1), it can be concluded that by adding DTAB in the electroless plating bath recipe, a pin-hole free Pd-composite membrane can be fabricated with significant reduction in Pd-film thickness and plating time.

To understand the role of DTAB surfactant, it will be useful to look into electroless plating reactions. Palladium deposition occurs according to the following two simultaneous reactions:

$$\text{Anodic Reaction}: N_2H_4 + 4OH^- \rightarrow N_2^{\uparrow} + 4H_2O + 4e^-$$

$$\text{Cathodic Reaction}: 2Pd[NH_3]_4^{2+} + 4e^- \rightarrow 2Pd^0 + 8NH_3^{\uparrow}$$

$$\text{Overall Reaction}: 2Pd[NH_3]_4^{2+} + N_2H_4 + 4OH^- \rightarrow 2Pd^0 + N_2^{\uparrow} + 8NH_3^{\uparrow} + 4H_2O$$

The cathodic deposition of Pd catalyzes the anodic oxidation of hydrazine resulting in an autocatalytic process. Pre-seeded Pd nuclei on the substrate during the sensitization/activation step reduce the induction period of the autocatalytic process at the beginning of the deposition. In these anodic and cathodic reactions, the ammonia and nitrogen gas bubbles formed are shown by the vertical arrowheads. These gas bubbles adhering to the substrate surface hinder deposition of Pd on the substrate surface and result in poor Pd film formation.

Using SIEP, DTAB played an important role in removing these gas bubbles from the surface. Tail groups of DTAB, which is hydrophobic in nature, appear to be aligned around the gas-liquid interface and form various spherical or cylindrical cage-like structures. DTAB also tends to form various meta-stable structures (spherical, cylindrical, or circular) at the solid-liquid interface that inherently helps finer grain formation and subsequent coarsening of the deposited film. Interaction of DTAB with a solid surface was investigated independently in hydrophobic glass surfaces. As shown in Fig. 3, the AFM image shows various cylindrical long chains but repetitive structure throughout the surface. This observation is in agreement with other published work (21). Further, DTAB may take part in the reaction kinetics. DTAB contain active bromide ions (Br^-) in the head group which is a strong oxidizing agent. This head group may participate in the reduction process of the complex salt and favorably take part in Pd grain formation and subsequent grain coarsening. These dual roles of DTAB appear to be very effective in thin film formation.

In CEP, besides the ionic strength of the reactants, the dendrite formation depends upon localized overpotentials, substrate morphology, bath recipe, and operating temperature. During the plating process, some Pd nuclei may grow faster than the others. This may be attributed to the plating thermodynamics and configurational limitations of the rough surface (11). Due to localized overpotentials, the driving force in electroless plating is not uniform, and as a result, metal seldom deposits uniformly throughout the surface. In Fig. 4, SEM images of a Pd-MPSS membrane

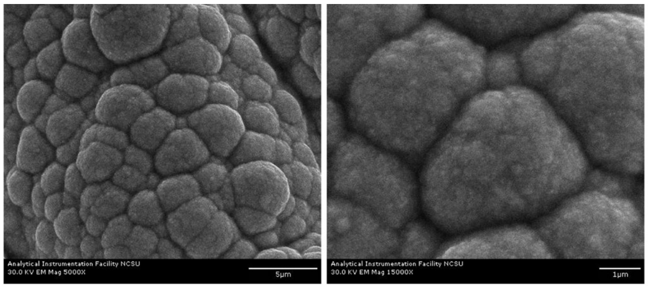

(a) SEM images of Pd-film in absence of DTAB (5k and 15k magnifications)

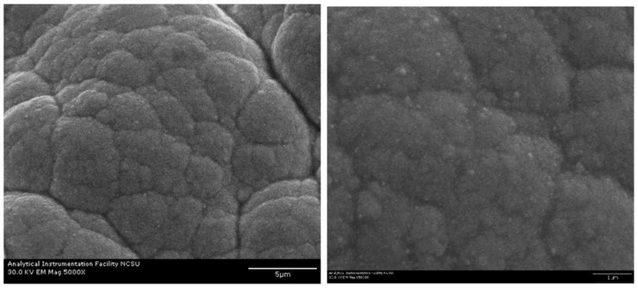

(b) SEM images of Pd-film in DTAB CMC×2 (5k and 15k magnifications)

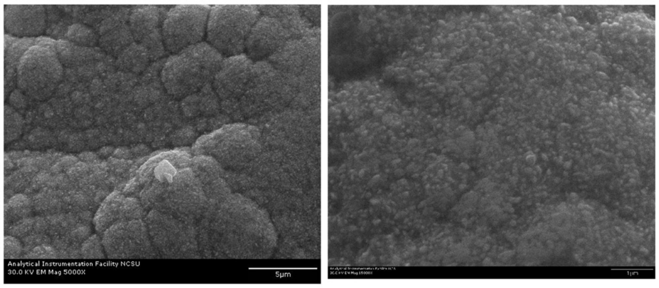

(c) SEM images of Pd-film in DTAB CMC×4 (5k and 15k magnifications)

FIG. 2. SEM images of membranes prepared by: (a) CEP, and (b and c) SIEP with DTAB as surfactant at CMC × 2 and CMC × 4, respectively.

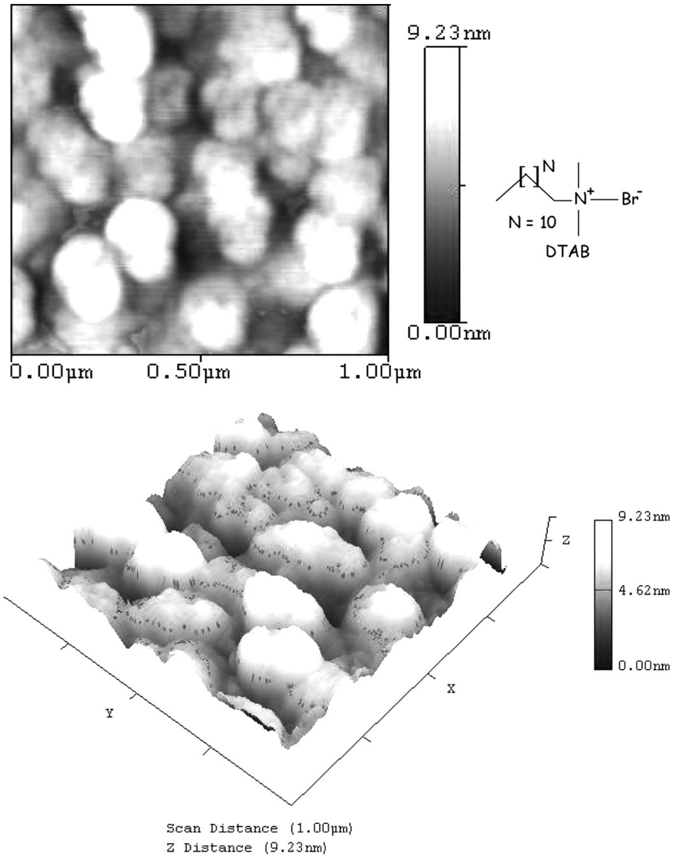

FIG. 3. AFM images of solid surface aggregation onto typical hydrophobic glass surface with DTAB.

that was fabricated by CEP is shown at two magnifications (5 k and 15 k). These images were taken after 20 minutes of the deposition cycle. It can be observed from the SEM images that Pd crystals form an uneven hillock of small dendritic grain over the surface. The formation and growth of dendrite is more pronounced at higher reaction kinetics. The Ag system is more reactive than Pd-system in electroless plating. In Fig. 5, the SEM images of Ag-MPSS membrane taken after 20-minutes of the deposition cycle using conventional electroless plating are shown. Like Pd grain formation (Fig. 4), Ag also forms a dendritic grain over the substrate surface. However, the Ag-MPSS grain structure is significantly finer than Pd-MPSS.

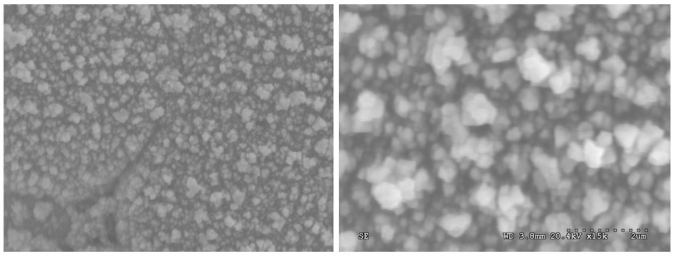

FIG. 5. Electroless plating observed after 20 minutes of deposition cycle showing initial dendrite growth Ag-deposition microstructures at 5 k and 15 k magnifications.

Non-uniformity in film deposition that results from dendrite nucleation is one of the major challenges in the fabrication of defect-free, thinner Pd-based membrane. Initial dendritic growth exists all over the substrate surface and hinders further uniform plating. The presence of a suitable surfactant in electroless plating may prevent the formation of dendrite by activating grain boundary migration. In this context, the role of DTAB in SIEP of Pd and Ag on MPSS was investigated. In Figs. 6 and 7, SEM images of Pd-MPSS and Ag-MPSS are shown after a 20-minute deposition cycle of SIEP. From the SEM images, it is observed that the dendrite formation is not visible after 20 minutes of deposition as compared to the images of Figs. 4 and 5 for Pd-MPSS and Ag-MPSS membranes, respectively. However, Ag-MPSS membrane has a smoother surface morphology as compared to the Pd-MPSS membrane. This is due to faster reaction kinetics of the Ag-system in the SIEP.

The effect of surfactant concentrations (DTAB in CMCs) on the Pd grain size is shown in Fig. 8 for electroless plating of Pd on MPSS in 20 minutes of plating. Using higher DTAB concentration, it is possible to deposit finer Pd grains on MPSS using SIEP. At a DTAB concentration of CMC × 4 the average Pd-grain size was reduced from

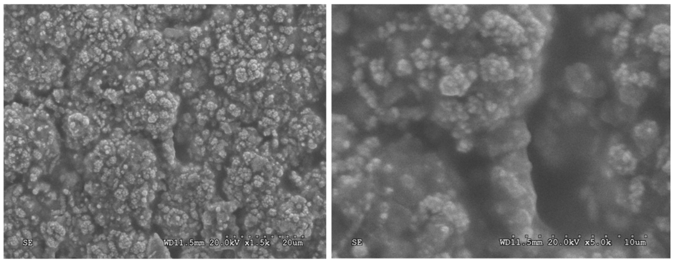

FIG. 4. Electroless plating observed after 20 minutes of deposition cycle showing initial dendrite growth in Pd-deposition microstructures at 5 k and 15 k magnifications.

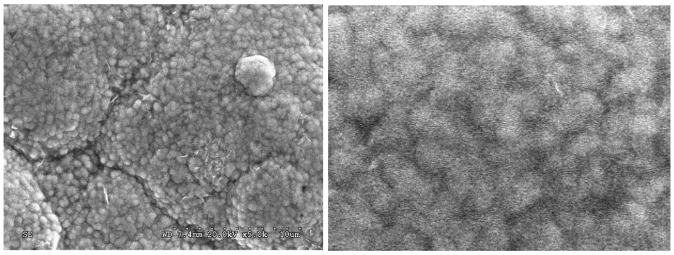

FIG. 6. Surfactant activated Pd deposition showing agglomerated grain growth throughout the surface (SEM images at 5 k and 15 k magnifications).

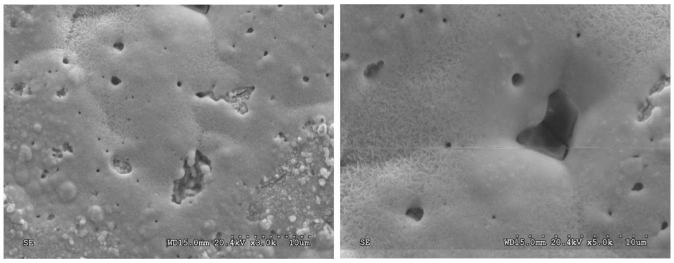

FIG. 7. Surfactant activated Ag deposition showing agglomerated grain growth throughout the surface (SEM images at 5 k and 15 k magnifications).

8 µm (without surfactant) to about 2 µm. To illustrate how DTAB influences the grain size, in Fig. 9 the grain size distribution (relative abundance, %) is compared as a function of the particle size for SIEP (DTAB at CMC × 1 and CMC × 4) and conventional electroless plating of Pd-MPSS in 20-minutes of deposition cycles. The particle size distributions clearly demonstrate that using DTAB in SIEP results in a significant reduction in Pd-grain size with an increased DTAB concentration.

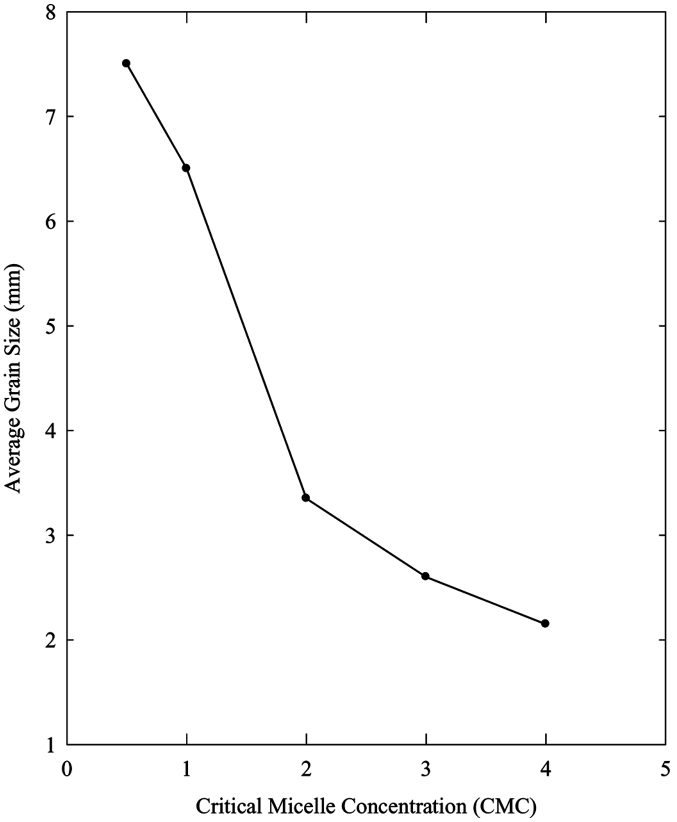

FIG. 8. Average grain size (µm) of Pd deposited in 20 minutes of plating (SIEP).

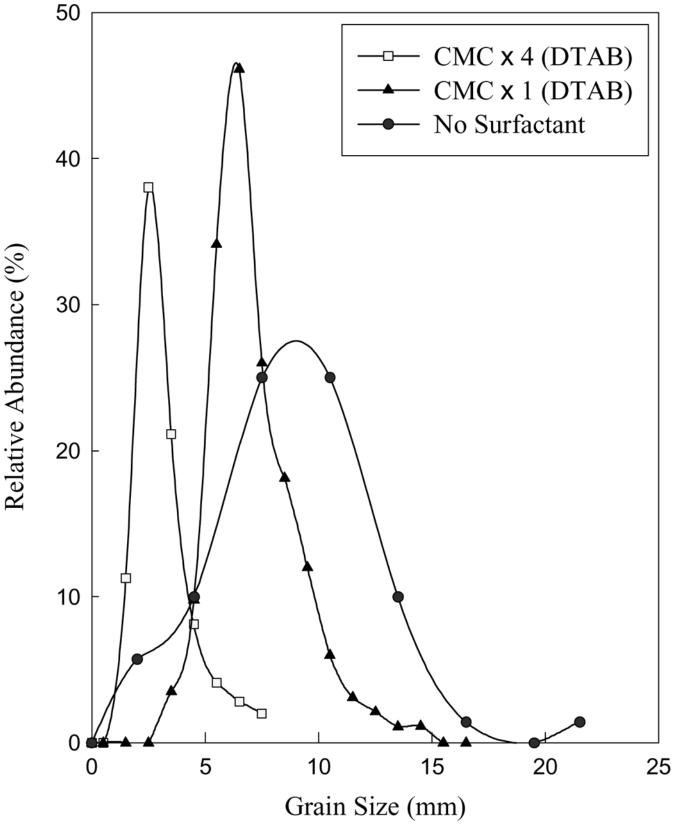

FIG. 9. Pd-grain size distribution observed in CEP (no-DTAB) and SIEP with DTAB at CMC × 1 and CMC × 4.

Surface elemental analysis carried out by energy dispersive spectroscopy (EDS) showed intense Pd peaks. Typical EDS analysis of Pd-film fabricated in DTAB surfactant is shown in Fig. 10. X-ray diffraction (XRD) showed peaks in [111], [200], [220], and [311], which imply the deposition of polycrystalline structure throughout the surface. Typical XRD spectra of Pd-peaks in DTAB surfactant is shown in Fig. 11. The EDS and XRD results of the Pd films fabricated by the CEP were very similar. By adding DTAB in the SIEP, no contamination was added to the Pd-film structure as confirmed by the EDS and XRD results.

From this study DTAB at CMC × 4 was found to be the most effective surfactant in SIEP that enabled the deposition of integrated, defect-free Pd film on MPSSS. The Pd-MPSS membranes fabricated by DTAB in SIEP were tested for gas-tightness and H_2 perm-selectivity in the permeability measurement set-up. The thickness of the Pd-film on MPSS support was found to be 7.68 µm as determined by the weight-gain method. The gas-tightness was measured using helium as the permeating gas through the membrane. Helium permeance was found to be $120\,m^3/m^2 \cdot hr$. The selectivity of hydrogen with respect to helium was about 1135 (20). This suggests the Pd-MPSS membrane fabricated by DTAB induced SIEP was extremely gas-tight and essentially defect-free at 7.68 µm Pd-film thicknesses. Thus,

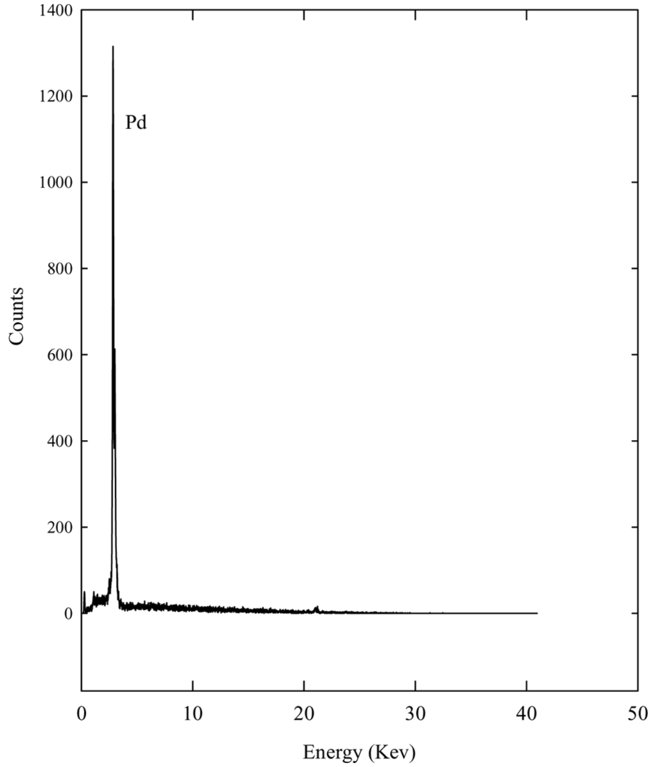

FIG. 10. Typical EDS analysis of Pd film fabricated by SIEP in DTAB.

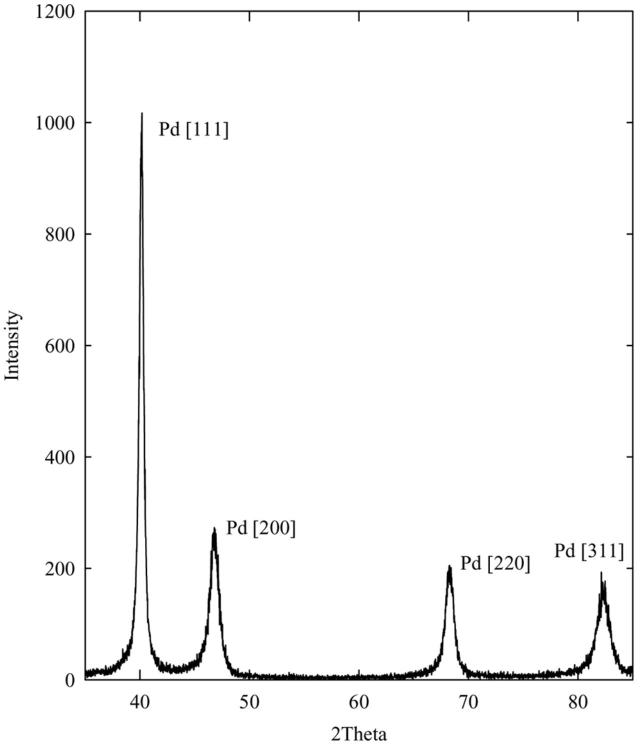

FIG. 11. Typical X-ray diffraction patterns of Pd-film fabricated by SIEP in DTAB.

by the SIEP method thinner membranes with better transport properties can be fabricated in less time.

CONCLUSIONS

A cationic surfactant (DTAB) was used in the electroless plating process to fabricate defect-free Pd-film on the MPSS substrate. The new method (SIEP) is an effective method of film fabrication with excellent control in grain formation and agglomeration. By manipulating the surfactant concentration (CMC) from 1 to 4, we were able reduce the Pd-film grain size from 8 µm to about 2 µm. The surface morphology as obtained by SEM images reveal significant grain fusion (agglomeration) in a surfactant activated deposition. The new Pd-MPSS membrane exhibited excellent H_2-permselectivity.

ACKNOWLEDGEMENTS

This research was sponsored by the U.S. Department of Energy – HBCU Program, under Award No. DE-FG26–05NT42492. Dr. Arun Bose, NETL, Pittsburgh, is the DOE Project Officer. However, any opinions, findings, and conclusions or recommendations expressed herein are those of the author and do not necessarily reflect the views of the DOE. Analytical support from the Center for Advanced Materials and Smart Structures (CAMSS) of North Carolina A&T State University is gratefully acknowledged with special thanks to Drs. Jag Sankar, D. Kumar, and Zhigang Xu.

REFERENCES

1. Jost, W. (1969) *Diffusion*; Academic Press: London, UK.
2. Uemiya, S.; Sato, N.; Ando, H.; Kude, Y.; Matsuda, T.; Kikuchi, E. (1991) Separation of hydrogen through palladium thin film supported a porous thin film. *J. Memb. Sci.*, 56: 303–313.
3. Jayaraman, V.; Lin, Y.S.; Pakala, M.; Lin, R.Y. (1995) Fabrication of ultrathin membranes on ceramic supports by sputter deposition. *J. Memb. Sci.*, 99: 89–100.
4. Jayaraman, V.; Lin, Y.S. (1995) Synthesis and hydrogen permeation properties of ultrathin palladium-silver alloy membranes. *J. Memb. Sci.*, 104: 251–262.
5. Bryden, K.J.; Ying, J.Y. (1995) Nanostructured palladium membrane synthesis by magnetron sputtering. *Materials Science and Engineering*, A204: 140–145.
6. Xomeritakis, G.; Lin, Y.S. (1998) CVD synthesis and gas permeation properties of thin palladium/alumina membranes. *AIChE J*, 44 (1): 174–183.
7. Nam, S.E.; Lee, K.H. (2005) Preparation and characterization of palladium alloy composite membranes with a diffusion barrier for hydrogen separation. *Ind. Eng. Chem. Res.*, 44: 100–105.
8. Shu, J.; Granddjean, B.P.A.; Neste, A.V.; Kaliaguine, S. (1991). Catalytic palladium-based membrane reactors: A review. *Can. J. Chem. Eng.*, 69: 1036.
9. Ma, Y.H.; Mardilovich, I.P.; Engwall, E.E. (2003) Thin composite palladium and palladium/alloy membranes for hydrogen separation. *Ann. N. Y. Acad. Sci.*, 984: 346–360.
10. Lu, G.Q.; Diniz da Costa, J.C.; Duke, M.; Socolow, R.; Williams, R.H.; Kreutz, T. (2007) Inorganic membranes for hydrogen

production and purification: A critical review and perspective. *J. Colloid and Interface Science*, 314: 589–603.

11. Souleimanova, R.S.; Mukasyan, A.S.; Varma, A. (2000) Effects of osmosis on microstructure of Pd-composite membranes synthesized by electroless plating technique. *J. Memb. Sci.*, 166: 249–257.
12. Roa, F.; Way, D.; McCormick, R.L.; Paglieri, S.N. (2003) Preparation and characterization of Pd-Cu composite membranes for hydrogen separation. *Chemical Engineering Journal*, 93: 11–22.
13. Goto, S.; Assabumrungrat, S.; Tagawa, T.; Prasethdam, P. (2000) The effect of direction of hydrogen permeation on the rate through a composite palladium membrane. *J. Memb. Sci.*, 175: 19–24.
14. Hou, K.; Hughes, R. (2002) The effect of external mass transfer, competitive adsorption and coking on hydrogen permeation through thin Pd/Ag membranes. *J. Memb. Sci.*, 206: 119–130.
15. Rothenberger, K.S.; Cugini, A.V.; Howard, B.H.; Killmeyer, R.P.; Ciocco, M.V.; Morreale, B.D.; Enick, R.M.; Bustamante, F.; Mardilovich, I.P.; Ma, Y.H. (2004) High pressure hydrogen permeance of porous stainless steel coated with a thin palladium film via electroless plating. *J. Memb. Sci.*, 244: 55–68.
16. Lee, D.W.; Lee, Y.G.; Nam, S.E.; Ihm, S.K.; Lee, K.H. (2003) Study on the variation of morphology and separation behavior of the stainless steel supported membranes at high temperature. *J. Memb. Sci.*, 220: 137–153.
17. Barton, J.L.; Bockris, J.O'M. (1962) The electrolytic growth of dendrites from ionic solutions. *Proceedings of the Royal Society of London. Series A, Mathematical and Physical Sciences*, 268 (1335): 485–505.
18. Ayturk, M.E.; Payzant, E.A.; Speakman, S.A.; Ma, Y.H. (2008) Isothermal nucleation and growth kinetics of Pd/Ag alloy phase via in situ time-resolved high-temperature X-ray diffration (HTXRD) analysis. *J. Memb. Sci.*, 316: 97–111.
19. Ilias, S.; Islam, M.A. (March 18, 2010) Methods of preparing thin films by elctroless plating. U.S. Patent Application 20,100,068,391.
20. Islam, M.A. (2008). The development of improved electroless plating in fabricating Pd-based membrane and membrane reactor application for hydrogen separation. Ph.D. Diss. North Carolina A&T State University.
21. Manne, S.; Gaub, H.E. (1995) Molecular organization of surfactants at solid-liquid interfaces. *Science*, 270: 1480–1482.